Sphingomyelinase acts by an area-activated mechanism on the liquid-expanded phase of sphingomyelin monolayers

Luisina De Tullio, Bruno Maggio, and María Laura Fanani[1]

Centro de Investigaciones en Química Biológica de Córdoba, Departamento de Química Biológica, Facultad de Ciencias Químicas, Universidad Nacional de Córdoba. Haya de la Torre y Medina Allende, Ciudad Universitaria, X5000HUA, Córdoba, República Argentina

Abstract **We describe the localization of Alexa-488-labeled SMase in SM/ceramide (Cer) lipid monolayers containing segregated liquid-condensed (LC) Cer-enriched domains surrounded by a continuous liquid-expanded (LE) SM-enriched phase. Langmuir-Schaefer films were made in order to visualize the labeled enzyme. Independently of initial conditions Alexa-SMase is preferably localized in the SM-enriched LE phase and it is not enriched at the domain boundaries. A novel mechanism is proposed for the action of SMase, which can also explain the regulatory effect of the surface topography on the enzyme activity. The homogeneous enzymatic generation of Cer in the LE phase leads to a meta-stable, kinetically trapped, supersaturated mixed monolayer. This effect acts as driving force for the segregation of the Cer-enriched domain following classical nucleation mechanisms. Accordingly, the number and size of Cer-enriched domains are determined by the extent of Cer supersaturation in the LE phase rather than by the SMase local activity. The kinetic barrier for nucleation, for which a compositional gap of at least 53 mol% of Cer is necessary to reach a thermodynamically stable LC phase, can explain the lag time to reaching full catalytic activity. Altogether, the data support an "area-activated mechanism," in which the enzyme is homogeneously active over the LE surface.**—De Tullio, L., B. Maggio, and M. L. Fanani. **Sphingomyelinase acts by an area-activated mechanism on the liquid-expanded phase of sphingomyelin monolayers.** ***J. Lipid Res.*** **2008.** 49: **2347–2355.**

Supplementary key words lipid phase coexistence • fluorescent-labeled sphingomyelinase • domain nucleation • ceramide • epifluorescence microscopy • lateral segregation • Langmuir-Schaefer films

Phospholipases are a group of mostly water-soluble enzymes, widely spread in nature, that perform their catalytic activity at an interface, owing to the insoluble nature of their substrates (1). Several studies have equated "membrane defects," such as those arising from the coexistence of lipid domains in different physical states, with enhanced catalytic activity (2–8). In 1990, it was reported that the liquid-expanded (LE), liquid-condensed (LC) lateral interfaces (lipid domain borders) in a one-component monolayer of 1,2-dipalmitoyl-*sn*-glycero-3-phosphocholine (DPPC) act as starting points for *Naja naja* phospholipase A_2 (PLA_2) catalytic activity (9). Dahmen-Levison, Brezesinski, and Mohwald (10) showed in lipid monolayers that the fluorescent-labeled PLA_2 preferably accumulates at the LC-LE interface of domains. Those results support the so-called perimeter-activated or border-activated mechanism, in which the enzyme must have physical contact with the domain boundary/membrane defect in order to become fully active and exerts its major catalytic action adsorbed to these linear interfaces (11). However, more recent studies (12) have demonstrated that fluorescein-labeled PLA_2 from *Crotalus atrox* was homogeneously distributed in 1-palmitoyl-2-oleoyl-phosphatidylcholine (POPC) and DPPC giant unilamellar vesicles when the lipids were in the LE state and preferentially localized in the LE phase at temperatures corresponding to the gel-fluid phase coexistence. The homogeneous distribution of PLA_2 on the membrane surface would support a mechanism by which the enzyme is fully active over the whole fluid surface (area-activated mechanism) but cannot adequately explain the enzyme activation by the presence of domain borders.

A group of phospholipases called SMases hydrolyze the membrane constituent SM to phosphocholine and ceramide (Cer), a modulator of membrane structure and dynamics

This work was supported by Secretaría de Ciencia y Tecnología- Universidad Nacional de Córdoba (SECyT-UNC), Consejo Nacional de Investigaciones Científicas y Técnicas (CONICET), and Fondo para la Investigación Científica y Tecnológica (FONCyT Argentina). B.M. and M.L.F. are career investigators of CONICET. L.D. is a doctoral fellow of CONICET.

Manuscript received 7 March 2008 and in revised form 8 May 2008.

Published, JLR Papers in Press, May 28, 2008.
DOI 10.1194/jlr.M800127-JLR200

Abbreviations: Cer, ceramide; $DiIC_{12}$, 1,1′-didodecyl-3,3,3′,3′-tetramethylindocarbocyanine perchlorate; DPPC, 1,2-dipalmitoyl-*sn*-glycero-3-phosphocholine; LC, liquid-condensed; LE, liquid-expanded; PLA_2, phospholipase A_2; POPC, 1-palmitoyl-2-oleoyl-phosphatidylcholine; X_{Cer}, mole fraction of ceramide.

[1] To whom correspondence should be addressed.
e-mail: lfanani@gmail.com

and a second messenger involved in cell signaling (13, 14). Previous studies in both lipid monolayers and bilayers have shown greater activity of SMase when the substrate is in a fluid state than when it is in the gel/ordered state (15–17). A detailed study of the time course of the SM degradation by SMase showed a correlation between the formation of Cer-enriched LC domains (immersed in a SM-enriched LE continuous phase) and the attainment of full catalytic capacity at the end of a lag period (18, 19). Recently, we showed how the initial presence of Cer-enriched LC domains favors precatalytic steps of SMase activation in a way that is dependent on the amount of the lateral interface present (20). These results point out that, similar to PLA_2, SMase action is also regulated by the presence of lateral membrane defects.

In this work, we investigated the mechanism of action of SMase, taking into consideration the border-activated versus area-activated alternative initially proposed for PLA_2. To this purpose, we studied the localization of *Bacillus cereus* SMase while it is actively hydrolyzing an initially pure SM film. Also, we examined the effect of the initial presence of lateral interfaces on the enzyme localization in mixed SM/Cer (9:1) monolayers in which LC domains and the LE phase coexist prior to the action of the enzyme. We found that SMase is preferably localized in the LE phase of the lipid monolayers. A mechanism is proposed on the basis of the area-activated mechanism for the enzymatic action of SMase that can also explain the regulatory effect of the surface topography. The proposed mechanism is analyzed integrating recent studies showing the influence of the initial presence of domains on SMase activity (20).

EXPERIMENTAL PROCEDURES

Chemicals

Bovine brain SM, bovine brain Cer, and *Bacillus cereus* SMase (EC 3.1.4.12) were purchased from Sigma-Aldrich (St. Louis, MO). The lipids were >99% pure by TLC and were used without further purification. The lipophylic fluorescent probe 1,1′-didodecyl-3,3,3′3′-tetramethylindocarbocyanine perchlorate ($DiIC_{12}$) and the amine-reactive probe Alexa Fluor 488 carboxylic acid succinimidyl ester were purchased from Molecular Probes (Eugene, OR). Solvents and chemicals were of the highest commercial purity available. The water was purified by the Milli-Q system to yield a product with a resistivity of ~18.5 MΩ/cm. Absence of surface-active impurities was routinely checked as described elsewhere (21).

Alexa dye conjugate of SMase

Conjugation of SMase with the dye was performed in 500 mM NaCl, 10 mM sodium phosphate, 1 mM $MgCl_2$ (pH 7.8). SMase was incubated with the amine-reactive dye Alexa Fluor 488 carboxylic acid succinimidyl ester, which was dissolved in DMSO and immediately added to the protein solution. The reaction mixture was incubated for 3 h in the dark, at room temperature under stirring, and stopped by diluting it with 100 mM Tris. The conjugated protein was purified from the unreacted dye by filtering through Centricon centrifugal filter 3000 (Millipore Corp.). Conjugates were labeled with an average ratio of 2:1 dye-protein molecule (calculated from absorbance measurements). A 15% (w/v) SDS-PAGE was used to verify the attachment of the dye to the protein. Protein bands were detected with Coomasie Brilliant Blue. Fluorescent bands were visualized by illumination of the gel with ultraviolet light in the dark. The labeled protein was stored in the dark at 4°C until use, and used without further dilution with unlabeled enzyme. Enzymatic assays showed that after being labeled, neither the lag time nor the rate of activity was changed, and the enzyme remained fully active, giving a two-dimensional specific activity of 300 ± 40 U/mg for the unlabeled SMase and 320 ± 20 U/mg for Alexa-SMase [the interfacial SMase concentration was calculated using the partition constant $Kp = 7 \times 10^4$ previously reported (22)].

Epifluorescence microscopy of monolayers

The monolayers SM and SM/Cer (9:1), without lipid fluorescent probe (SMase-Alexa 488 experiments) or with 1 mol% $DiIC_{12}$ (lipophylic probe that preferentially partitions into the LE phase), were spread from preformed lipid solutions in chloroform-methanol (2:1) over a subphase of 10 mM Tris/HCl, 125 mM NaCl, 3 mM $MgCl_2$, pH 8 until reaching a pressure of less than ~0.5 mN/m. After solvent evaporation (10 min), the monolayer was slowly compressed to the desired surface pressure (10 mN/m).

Alexa-SMase (final concentration 10 mU/ml) or unlabeled SMase (final concentration 0.5–7 mU/ml) was injected into the subphase of a circular reaction compartment (3 ml; 3.14 cm^2). The all-Teflon zero-order trough (Kibron μ-Trough S; Kibron, Helsinki, Finland) was mounted on the microscope stage. Epifluorescence microscopy was carried out (Zeiss Axiovert 200 or Zeiss Axioplan; Carl Zeiss, Oberkochen, Germany) using a mercury lamp (HBO 50), a 20× LD objective, and a rhodamine-fluorescein filter set. Images with exposure times between 1 and 2 s (Alexa 488-labeled monolayers), were recorded with a CCD video camera (Zeiss) controlled by Axiovision 3.1 software. Images with exposure times of 60 ms ($DiIC_{12}$-labeled monolayers) were recorded with a CCD video camera controlled by Metamorph 3.0 software. All experiments were carried out in an air-conditioned room (22 ± 2°C).

Preparation of Langmuir-Schaefer films

Coverslips (12 mm-diameter) were first alkylated with octadecyltrichlorosilane to self-assemble a covalently linked monolayer of octadecylsilane. The coverslips were precleaned in hot piranha solution (1 vol 30% H_2O_2; 3 vol H_2SO_4) for 1 h (Warning: piranha solution reacts violently with organic materials). The quality of hydrophobic coverage of each coverslip was routinely checked before use. Monolayers were transferred from the air-water interface to solid supports. To perform the transference, the coverslip was held above the monolayer and slowly lowered until touching it (23). After a few seconds, the coverslip was pushed through the monolayer. Coverslips were gently washed before being observed through the microscope (always maintained under aqueous solutions to avoid collapse of the monolayers). At least two independent samples were imaged for each monolayer composition.

Determination of enzymatic activity

Details of the equipment used have been given elsewhere (18). Briefly, an adjacent compartment (connected to the reaction compartment through a narrow and shallow slit) serves as a substrate reservoir in order to maintain constant surface pressure during the enzymatic reaction. Because Cer remains at the interface, and owing to the difference of cross-sectional area between SM and Cer (~84 $Å^2$ and 51 $Å^2$ at 10 mN/m, respectively), the enzymatic activity can be determined by continuously recording the reduction of the film area as a function of time (24).

Assessment of the mole fraction of Cer on the LC phase from epifluorescence images of SM/Cer monolayers

From epifluorescence micrographs of mixed SM/Cer monolayers originally published in (18) and shown in **Fig. 1A–F**, we extracted information about the area fraction occupied by the LC phase at different Cer content. Figure 1G shows a linear dependence of the area fraction occupied by the LC phase with the content of Cer in the film (X_{Cer}^{t}). The variation of the LC area fraction (Δfc^{LC}) is defined in equation 1 as follows:

$$\Delta fc^{LC} = \Delta a / a^{t} \qquad (Eq.\ 1)$$

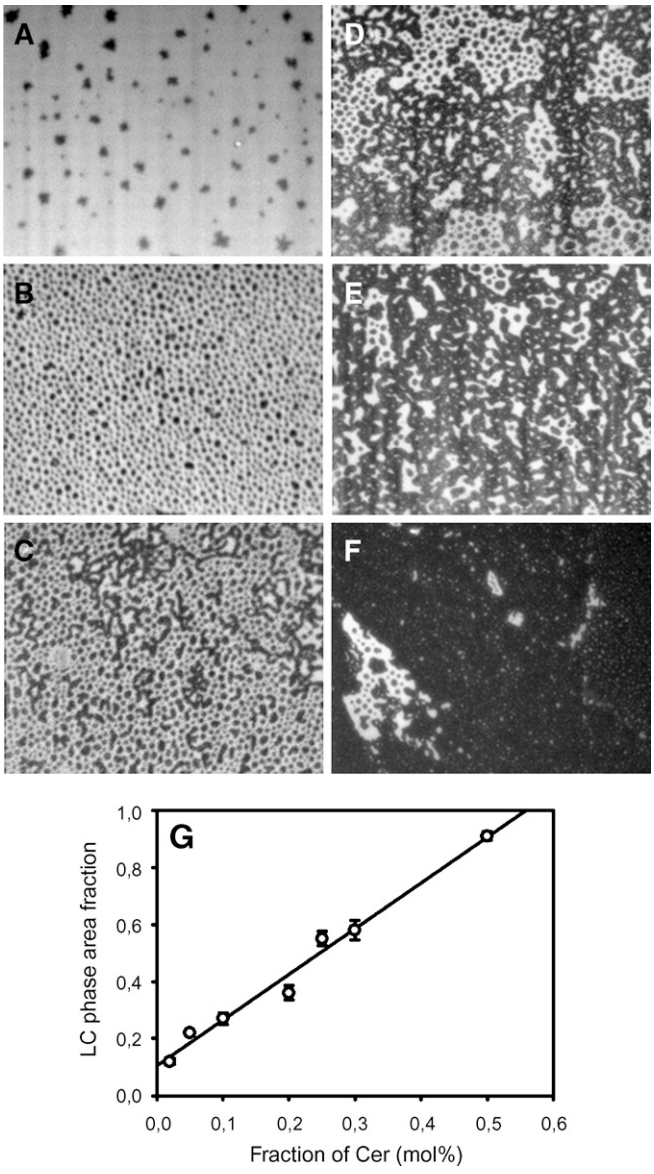

Fig. 1. Correspondence of the area fraction occupied by the liquid-condensed (LC) phase and the ceramide (Cer) content on mixed SM/Cer monolayers. A–F: Epifluorescence micrographs of 1,1′-didodecyl-3,3,3′,3′-tetramethylindocarbocyanine perchlorate ($DiIC_{12}$)-labeled premixed SM/Cer monolayers at 10 mN/m of surface pressure containing 2, 10, 20, 25, 30, and 50 mol% of Cer, respectively. Image size 225 × 175 μm [from (18) with kind permission of the Biophysical Society]. G: Linear dependence of the LC phase area fraction with the content of Cer at the interface. Error bars represent SEM.

Δa is the change of area occupied by the LC phase, and a^{t} the total area of the analyzed image. Δa is related to the number of Cer molecules per frame that are added to the system (Δn_{Cer}), shown in equation 2 as follows:

$$\Delta a = \Delta n_{Cer} \cdot \bar{A}_{Cer} + \Delta n_{SM}^{LC} \cdot \bar{A}_{SM}^{LC} \qquad (Eq.\ 2)$$

Δn_{SM}^{LC} is the number of SM molecules per frame that partition into the LC phase as a consequence of an increase of Cer in the system, and $\bar{A}_{Cer}$ and $\bar{A}_{SM}^{LC}$ are the average molecular area of Cer and SM, respectively, in the LC phase. SM is assumed to be in a condensed state when becoming integrated into the LC domains, and its mean molecular area is calculated as an extrapolation of the condensed portion of the known isotherm curve [Fig. 1 in (18)] to lower surface pressures.

The newly added molecules of Cer are assumed to be segregated from the Cer-saturated LE phase; therefore, in equation 3,

$$\Delta n_{Cer} = \Delta X_{Cer}^{t} \cdot n^{t} \qquad (Eq.\ 3)$$

ΔX_{Cer}^{t} is the total change of the Cer mole fraction in the system and n^{t} the total number of molecules per frame. In equation 4, n^{t} is calculated as

$$n^{t} = a^{t} \Big/ \bar{A}_{av} \qquad (Eq.\ 4)$$

$\bar{A}_{av}$ is the experimental average molecular area of the mixed SM/Cer monolayer. Taking into account that the Cer mole fraction in the LC phase can be expressed as shown in equation 5,

$$X_{Cer}^{LC} = \frac{\Delta n_{Cer}}{\Delta n_{Cer} + \Delta n_{SM}^{LC}} \qquad (Eq.\ 5)$$

and using equations 2 and 3, we can calculate X_{Cer}^{LC} as 0.53 ± 0.06 (SEM) for the premixed monolayers and 1.1 ± 0.1 (SEM) for the monolayer under SMase activity.

RESULTS

SMase-induced formation of Cer-enriched (LC) domains

As reported previously, SMase-induced SM→Cer conversion on SM monolayers leads to the formation of LC Cer-enriched domains (18). The activity of SMase shows a lag time period followed by a constant rate (steady-state) period and a slow halting of the reaction owing to product accumulation at the interface [**Fig. 2A** and (22)]. With the aid of $DiIC_{12}$, a lipophylic probe that selectively partitions into LE phases, it is possible to distinguish between SM-enriched LE (bright area in Fig. 2B–E) and Cer-enriched (LC) phases (dark domains in Fig. 2B–E). As was reported previously in detail (18, 19), the SMase action against a pure SM monolayer, which shows initially a homogeneous LE phase (see Fig. 2B), induces the formation of small circular domains at the end of the lag time period that grow steadily during the constant rate of the reaction (Fig. 2C). The enlargement of the Cer-enriched (LC) domains leads to successive domain shape transitions to increasingly branched morphologies (see Fig. 2C) that can be explained by Möhwald/McConnell shape transition theory (25, 26). Within this theoretical framework, the branched domain morphology appears to be a consequence of intradomain electrostatic repulsion owing to the progressive enrichment within the domain lipid with a considerable dipole moment

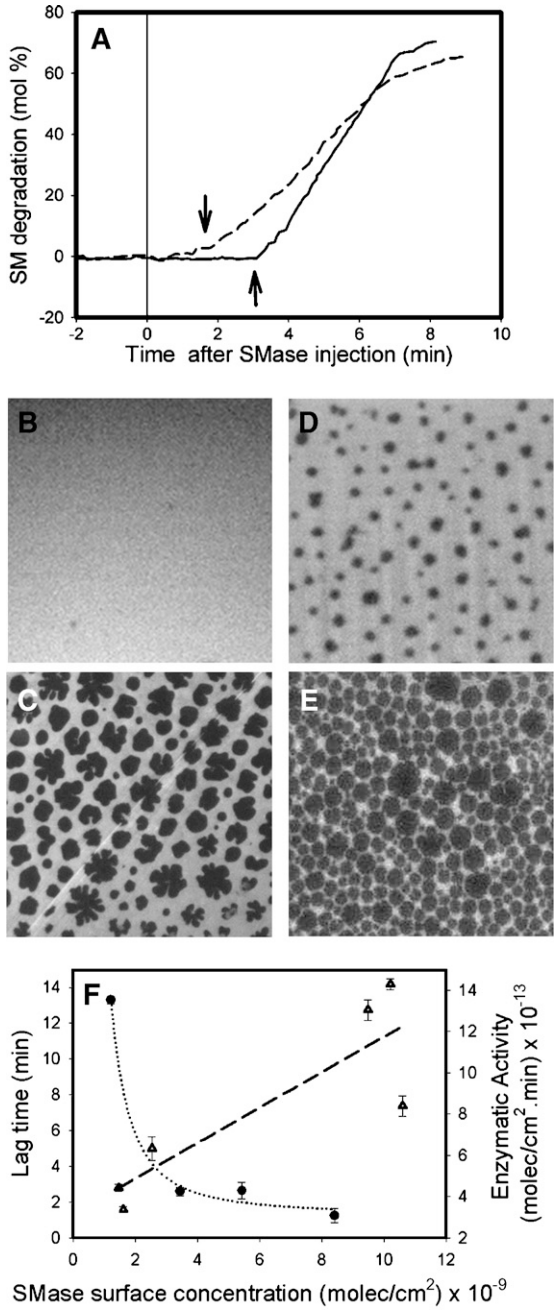

Fig. 2. Topographical properties of SMase-driven SM→Cer conversion. A: Time course of SM to Cer conversion by SMase acting on an initially pure SM monolayer (unbroken line) or premixed SM/Cer (9:1) monolayer (dashed line). The arrows indicate the beginning of the constant rate regime [reprinted from (20) with kind permission of Springer Science and Business media]. B–E: Epifluorescence micrographs of $DiIC_{12}$-labeled lipid monolayers (actual size 140 × 140 μm). The bright regions ($DiIC_{12}$-enriched) denote LE, SM-enriched phase, whereas the dark areas ($DiIC_{12}$-depleted) are liquid-condensed Cer-enriched domains. B, D: Air/water monolayers containing pure SM (B) or SM/Cer (9:1) (D) (before SMase injection). C, E: Topographic pattern of transferred (Langmuir-Schaefer) monolayer under the action of SMase in the constant rate period acting on initially pure SM (C) or SM/Cer (9:1) (E) films. F: Lag time (closed circles) and enzymatic activity dependence (open triangles) with SMase surface concentration [(molecules/cm^2) × 10^9; taken from (22)]. [For details regarding topographic evolution of SMase-generated Cer-enriched domains see (19, 20)].

such as Cer. Concomitantly with this shape transition process, a long-range ordering of domains in a hexagonal lattice is established as a consequence of long-range interdomain electrostatic repulsion (19).

When SMase acts on an interface that initially contains Cer [SM/Cer (9:1)], and therefore, initially presents Cer-enriched (LC) segregated domains (Fig. 2D), the reaction curve shows a shorter lag time and a lower catalytic rate [Fig. 2A and (15)]. Under these conditions, the SMase-generated, Cer-enriched domains evolve with more rounded morphologies than when the enzyme is initially acting on pure SM films [cf. Fig. 2C, E and see also (20)]. It is worth noting that the difference in the kinetic behavior between the two conditions [SM and SM/Cer (9:1)] cannot be explained as a simple difference of the enzyme partitioning to the interface, on the basis of the detailed analysis of the different kinetic steps of the action of SMase on SM monolayers that was previously reported (22). As shown in Fig. 2F, the lag time period decays inversely with the amount of adsorbed enzyme, whereas the catalytic rate in the constant rate period increases linearly. Thus, neither a higher nor a lower amount of SMase adsorbed onto the SM/Cer (9:1) interface, compared with the action on pure SM, can explain the kinetic difference observed. De Tullio et al. (20) reported that the end of the lag time appears to be related to a same fixed amount of domain border per frame for both cases, pure SM or SM/Cer (9:1), even though this stage is reached over different times.

Surface localization of SMase

Important questions are whether SMase is located along the domain borders or acts evenly distributed in one of the two phases present, and how this distribution might affect its kinetic properties. Therefore, enzyme localization appears to be key data for interpretation of the mechanism of enzyme regulation by the presence of domain borders. To address these questions, we studied by epifluorescence microscopy the localization of Alexa-labeled SMase during its action on both initially pure SM and mixed SM/Cer (9:1) monolayers. SMase visualization was achieved both at the air-water interface and by transferring the monolayer to a solid support by the Langmuir-Schaefer method. SMase was injected into the subphase of pure SM or SM/Cer (9:1) monolayers, and the SM→Cer conversion was allowed to occur until the constant rate period was established. For the observation of the enzyme associated with the monolayers, it was necessary to extensively perfuse the subphase with a dual syringe pump for simultaneous infusion and withdrawal in order to eliminate the considerable amount of background fluorescence remaining in the subphase. Monolayers transferred as Langmuir-Schaefer films, allowing washing and better elimination of subphase background, showed a pattern similar to that of the air-water monolayers (not shown) but in immobile, higher quality images.

Figure 3A, B shows images of Langmuir-Schaefer films of Alexa-SMase acting on initially pure SM monolayers when about ≈20–30% (Fig. 3A) or ≈50–60% (Fig. 3B) of the SM substrate was hydrolyzed to Cer. The images show a more intense labeling in the continuous phase than in the

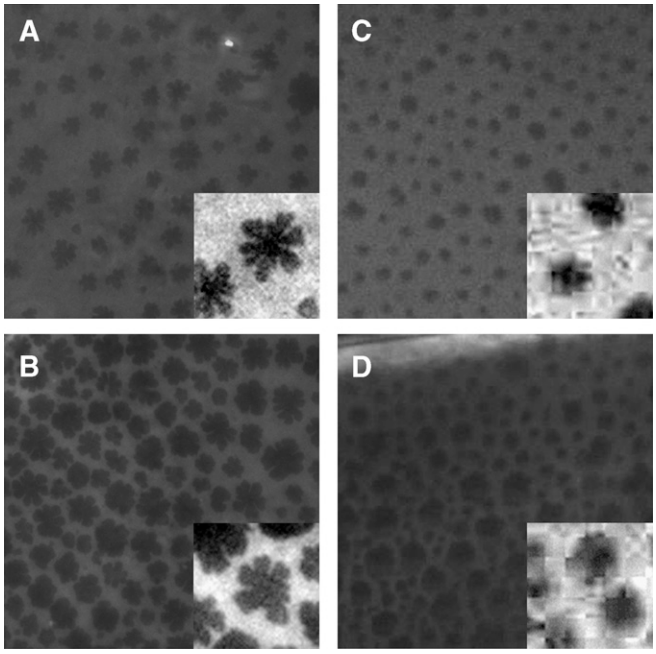

Fig. 3. Surface localization of Alexa-labeled SMase. Representative epifluorescence micrographs of Alexa-SMase-labeled transferred monolayers are shown acting on initially pure SM monolayers (A, B) or initially mixed monolayers of SM/Cer (9:1) (C, D). Images were taken at the beginning of the constant rate period (~20–30% of SM hydrolized) (A–C) or at the end of the constant rate period (~50–60% of SM hydrolyzed) (B–D). No lipid probe was used in these experiments. Images with further-enhanced contrast (insets) show that the labeling is not enriched at the domain borders, within the sensitivity of the method. Image size is 140 × 140 μm for all panels except insets, which are 23 × 23 μm.

domains. Insets in Fig. 3 show expanded, contrast-enhanced images showing that the labeling is not preferentially enriched at the domain borders. Comparison of images in Fig. 3A, B with Langmuir-Schaefer transferences of unlabeled SMase acting on SM/$DiIC_{12}$ (1 mol%) monolayers (Fig. 2C) supports the assignment of an LE state to the Alexa-SMase-enriched (continuous) phase. Altogether, we found that the Alexa-SMase preferably locates in the LE ($DiIC_{12}$-enriched) phase and, within the sensitivity of the method, we could not detect preferential enrichment at the lateral interfaces of the domains (see inset in Fig. 3A, B). The initial presence of lateral interface on the substrate monolayer does not alter the distribution of SMase. Alexa-SMase acting on the SM/Cer (9:1) monolayer also preferentially partitions homogeneously into the continuous phase (Fig. 3C, D), which can be assigned as the LE phase by the $DiIC_{12}$ partition preference (Fig. 2E). This indicates that the initial presence of lateral interfaces does not favor a detectable enrichment of the enzyme at the domain boundaries.

Dependence of size and number of Cer-enriched (LC) domains on the enzymatic catalytic rate

To understand the mechanism of SMase-induced domain formation, we studied the changes of topographic features of (initially pure SM) monolayers induced by different amount of SMase added to the subphase. **Figure 4A–D** shows qualitatively that the larger the amount of enzyme added to the subphase, the higher the number of smaller Cer-enriched (LC) domains formed during the constant rate period. Because the SMase catalytic rate in this period is linear with the enzyme subphase concentration (22), the number of domains formed can be analyzed as a function of the Cer production rate (Fig. 4E). In addition, as the catalytic rate slows, the size of the domains becomes larger (Fig. 4F). **Table 1** shows detailed data about the experiments analyzed in Fig. 4 plus additional experiments performed in the absence of the cofactor Mg^{2+}. Under this condition, a larger number (20-fold) of SMase molecules are necessary to reach a catalytic activity similar to that of control ($+Mg^{2+}$) experiments. From the analysis of Table 1, we can conclude that the number of domains per frame correlates better with the SMase catalytic activity than with the amount of SMase molecules at the interface. The significance of these observations is discussed below.

DISCUSSION

Estimation of the composition of the LC and LE phases in premixed and SMase-induced SM/Cer monolayers

To explore alternative mechanisms for the activation of SMase induced by the domain lateral interface, we analyzed in depth the details of the SM/Cer demixing process. Premixed SM/Cer monolayers at the surface pressure used in this work (10 mN/m) show the presence of Cer-enriched LC domains over the composition range 0.02–0.5 mole fraction of Cer (X_{Cer}) [the epifluorescence images were initially published in (18) and are shown in Fig. 1]. Below $X_{Cer} = 0.02$, the monolayer is formed by a homogeneous LE phase. In the range of X_{Cer} 0.02–0.3, Cer-enriched LC domains are present immersed in a continuous LE phase (Fig. 1A–C). Above $X_{Cer} = 0.3$, the LC phase becomes the continuous phase delimiting LE isolated domains (Fig. 1D, E). At $X_{Cer} = 0.5$, the LC phase covers 91 ± 2% of the total area (Fig. 1F). The extent of the LC phase clearly exceeds the area occupied by Cer; thus, the LC phase must consist of a mixture of SM and Cer. Under conditions in which Cer is enzymatically generated by SMase, a lower fraction of area is occupied by the LC phase at the same SM/Cer composition, and this reflects an increased enrichment of Cer in the LC segregated domains (18). A minimal amount of Cer is also present in the LE phase. This is evidenced from the observation that monolayers with a content of Cer lower than $X_{Cer} = 0.02$ show a homogenous LE phase. This indicates that the mixed monolayers of SM/Cer can be described in the micrometer range as a heterogeneous coexistence of two separate but mixed phases, an SM-enriched LE phase and a Cer-enriched LC phase.

An estimation of the composition of the LC phase can be performed taking into account the molecular areas occupied by Cer and SM in the LC state and the experimental average molecular area of the mixed monolayers (see Materials and Methods for details). According to the calculations described in the Materials and Methods section, the segregated LC phase domains contain an estimated lipid

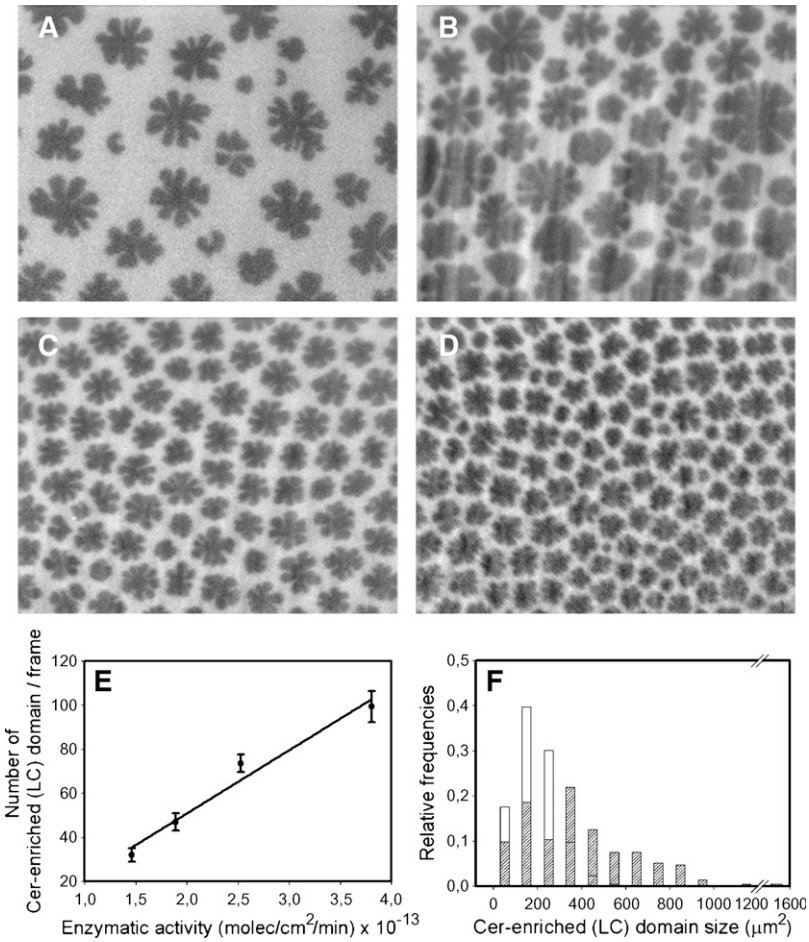

Fig. 4. Relationship between the number and size of Cer-enriched domains per frame with SMase catalytic rate. A–D: Fluorescence representative images of initially pure SM monolayers labeled by 0.5 mol% of $DiIC_{12}$ under the action of SMase (at the end of the constant rate period) at different SMase enzymatic rates expressed as molecule/cm^{-2}/min^{-1} × 10^{13} ± SEM. A: 1.5 ± 0.3. B: 1.9 ± 0.4. C: 2.5 ± 0.5. D: 3.8 ± 0.8. Image size is 225 × 175 μm for all cases. E: Number of Cer-enriched domains per frame at different SMase catalytic rates (linear range regarding SMase subphase concentration). The error bars represent the SEM. F: Histograms of the relative frequencies of domain size for the conditions illustrated in Fig. 4A, D corresponding to the fastest (open bars) and slowest (striped bars) SMase catalytic rate.

composition of $\sim X_{Cer} = 0.53 \pm 0.06$ (SEM) immersed in a continuous SM-enriched LE phase containing $< X_{Cer} = 0.02$. The same analysis for monolayers in which Cer was generated enzymatically by SMase gives a mole fraction of Cer in the LC domains close to unity.

SMase acts homogeneously on the SM-enriched (LE) continuous phase

Our results indicate that Alexa-SMase is preferably partitioned in the LE phase. This is in keeping with previous work reporting a preference of SMase for the substrate

TABLE 1. Correlation between the number of Cer-enriched (LC) domains and the amount of adsorbed SMase

SMase in Subphase[a] (Molecules/cm^{-3}) × 10^{10}	Adsorbed SMase[a,b] (Molecules/cm^{-2}) × 10^{9}	Enzymatic Activity (Molecules/cm^{-2}/min^{-1}) × 10^{13} ± SEM	Number of Cer-enriched (LC) Domains per Frame[c] ± SEM	SMase per LC Domain (Molecules × 10^{4}) ± SEM
7.52	1.5	1.5 ± 0.3	32 ± 3	1.9 ± 0.3
22.6	4.52	1.9 ± 0.4	47 ± 4	3.8 ± 0.7
45.16	9.04	2.5 ± 0.5	74 ± 4	4.8 ± 0.7
90.33	18.1	3.8 ± 0.8	99 ± 7	7.2 ± 1.13
953.5[d]	190.9	2.5 ± 0.1	126 ± 4	60 ± 6.9

LC, liquid-condensed.
[a] SEM values are below 9%.
[b] Adsorbed SMase concentration was calculated using the partition constant (Kp = 7 × 10^{4}) determined in (22).
[c] Image frame is 225 × 175 μm size.
[d] Experiment performed in the absence of the cofactor Mg^{2+} in order to work under slow catalytic conditions.

when it is in the fluid state compared to gel/ordered states (15–17, 27). In our previous work (20), we suggested the possibility that the presence of lateral interface could be involved in the completion of the precatalytic steps necessary for the enzyme to reach the steady-state condition (constant rate period). However, our present results testing that hypothesis indicate that the enzyme is homogeneously distributed in the LE phase and does not preferentially concentrate at the lateral interface of the domains. Thus, a direct physical influence of the lateral interface on the enzyme catalytic properties is not straightforward. On the other hand, the possibility that enzyme molecules in contact with the lateral interface could be more active, even though the enzyme is distributed homogeneously in the LE phase, can also be ruled out with our results. If the enzyme acts preferably at the domain boundaries, the catalytic rate should depend directly on the total amount of lateral interface. In previous work, we demonstrated that the amount of lateral interface increases during the constant rate period of SM degradation by SMase (period of domain growth), whereas the reaction rate remains constant until a sudden drop in activity occurs owing to domain percolation (and LE phase disconnection) (19). Thus, no direct correlation can be established between the amount of lateral interface and the reaction rate.

Perimeter-activated versus area-activated mechanism of action for phospholipases

For the largely studied reaction catalyzed by PLA_2-type enzymes, a literature search shows that the mechanism of action on a lipid organized surface in which LE-LC coexistence is present cannot be definitely established. In two different studies (9, 28), it was reported that the enzyme caused substrate degradation of the LC domains beginning from the domain boundary. However, a close analysis reveals that the methodology used in those studies cannot actually ascertain whether the LE phase was not likewise degraded, because substrate degradation within the LE phase cannot be distinguished by the probe used. Atomic force microscopy monitoring of PLA_2 degradation of DPPC over a solid support confirmed the data that the enzyme initiates the degradation of the substrate in an LC state from the lateral defects of intermolecular packing in lipid bilayers (7) but cannot assess the degradation mechanism in an LC-LE interface. Dahmen-Levison, Brezesinski, and Mohwald (10) showed that fluorescein-labeled PLA_2 actually accumulates preferentially at the LC-LE interface. Conversely, and more recently, Sanchez et al. (12) demonstrated that fluorescein-labeled PLA_2 from *C. atrox* was homogeneously distributed in POPC/DPPC giant unilamellar vesicles when the lipids were in the LE state and preferentially localized in the LE phase in mixed lipid giant unilamellar vesicles at temperatures corresponding to the gel-fluid phase coexistence. However, in these studies, catalytic activity was not assessed, and whether the enzyme adsorbed to the lateral interface is more active than the enzyme adsorbed to the bulk LE phase could not be ascertained. Recent attempts to clarify this point were made by Simonsen, Jensen, and Hansen (11). They followed the enzymatic hydrolysis by PLA_2 of POPC bilayer islands in the LE state through the reduction of the total substrate-supported bilayer. In that work, the authors proposed a kinetic model to discriminate between a perimeter-activated and an area-activated mechanism. The kinetic constants obtained showed a higher catalytic rate for the perimeter-activated compared with the area-activated model. The authors concluded that their results could support that the enzyme activation occurred along the island boundaries. Nevertheless, it was also shown that both model mechanisms were able to fit the kinetic data. On the other hand, when the bilayer islands underwent discrete jumps of perimeter length but not of area, the reaction rate remained smooth. This observation would be contrary to the perimeter-activation mechanism but can support the idea of the reaction taking place over the island surface (area-activated mechanism).

Kinetic barrier for nucleation of Cer-enriched domains as a regulatory mechanism for SMase activity at the interface

In the present work, based on the homogeneous localization of SMase in the LE phase and on the former calculation of the Cer content in the LC phase, we advance a novel mechanism for SMase regulation by the surface topography that can integrate the data available. Under this interpretation, the homogenous enzymatic generation of Cer in the LE phase leads to a meta-stable, kinetically trapped, supersaturated mixed monolayer (the thermodynamically stable mixture contains $X_{Cer} = 0.02$; see Discussion). Because the presence of Cer in the monolayer inhibits the enzymatic activity [see Fig. 2A and (15, 20)], the mechanism may involve a product-induced inhibition of the SM→Cer conversion within the LE phase. When the initial monolayer (reaction time = 0) does not show laterally segregated domains (pure SM monolayers, Fig. 2B), occurrence of nucleation events is necessary in order to cause large-scale demixing and the formation of a two-phase system in the monolayer. After a lag time in which domain nucleation occurs [with the reaction taking place at a low rate of enzymatic activity (18)], the excess Cer molecules become segregated into the LC domains and the Cer content in the LE phase approaches the equilibrium value (i.e., $<X_{Cer} = 0.02$). Under this condition, the enzyme is able to reach full catalytic properties and the reaction enters the steady-state condition (20).

The Cer supersaturation in the LE phase would act as driving force for nucleation of Cer-enriched domains, as shown in equation 6, according to the classic nucleation mechanism (29, 30):

$$\Delta G = -n\Delta\mu + 2\pi r\lambda \qquad (Eq.\ 6)$$

where n is the number of molecules in the nucleus seed, r is the radius of the circular nucleation seed, $\Delta\mu$ is the chemical potential difference between the two phases (that depends on how far from equilibrium the system is), and λ is the line tension between the two phases. As predicted by classical nucleation theory (equation 6), the number of stable nuclei increases as the driving force grows; in this

case, the driving force is the degree of supersaturation within the LE phase ($\Delta\mu$). Equation 6 also indicates that nucleation and growth of domains are opposed by linear tension, being necessarily the formation of a nucleus of n large enough to overcome the second unfavorable term of the equation. This effect adds extra energy requirements for the enlargement of the lateral interface and the formation of a stable nucleus (29, 31). The occurrence of compositional fluctuations necessary to form droplets of the new phase, large enough to overcome line tension, is a kinetically dependent process. In the present case, the compositional gap to reach a stable LC phase is proposed to be $\sim X_{Cer} \geq 0.53$, depending on how near the system is to equilibrium conditions (see Discussion). The proposal of classical nucleation theory as the mechanism for domain formation is supported by the experimental data. Taking the Cer supersaturation in the LE phase as the driving force for nucleation ($\Delta\mu$), the faster the Cer is produced, the further from equilibrium (supersaturation) should be the concentration of Cer in the LE phase. Under these conditions, the driving force becomes larger, and additionally, compositional fluctuations are more likely to occur in order to reach the compositional gap necessary for overcoming the line tension and the formation of stable nuclei. Therefore, at high enzymatic rates, a larger number of Cer-enriched LC domains at the end of the steady-state period should be expected. This expectation is satisfied as shown in Fig. 4E and Table 1. Concomitantly, at high enzymatic rates with fast Cer production, Cer molecules should partition into a large number of nuclei, leading to the formation of many small domains, whereas at low Cer production rates, few large domains would be formed (Fig. 4F). An alternative interpretation of the results shown in Fig. 4 could also be hypothesized. The physical presence of the enzyme, or the local production of Cer at the interface could be influencing/inducing nucleation of new domains, and therefore a higher number of SMase molecules (and not only the overall Cer production rate) might result in a larger number of domains. To test this interpretation, 20-fold more total enzyme concentration in the subphase was used in the absence of the cofactor Mg^{2+} (compared with the activity in its presence) in order to reach similar catalytic rates during the steady-state period (Table 1). Despite the large difference in the enzyme amount, the number of Cer-enriched domains per frame only doubled. Additionally, the results given in Table 1 show that the relationship between the amount of adsorbed SMase molecules and domains per frame is not constant among different experiments (see SMase per LC domain column in Table 1). The number of domains per frame appears to be related to the enzymatic activity rather than to the number of adsorbed SMase molecules (Table 1). Therefore, the nucleation of Cer-enriched domains does not appear to be a direct consequence of the formation of Cer in localized spots, but rather of the extent of Cer supersaturation in the LE phase.

When lipid domains are initially present in the substrate monolayer [initial monolayer for SM/Cer (9:1), see Fig. 2D], the Cer molecules homogenously produced in the LE phase can become immediately excluded by partitioning into the preexisting domains, which decreases supersaturation of Cer in the LE phase. In a previous work (20), we reported that SMase acting on SM/Cer (9:1) films induced the continuous enlargement of an almost unchanged number of LC domains throughout the reaction. Thus, most of the newly generated Cer molecules are essentially destined for the growth of the preexisting LC domains and not for the generation of new nuclei. Thus in this case, the kinetic barrier for nucleation is not present and the lag time period necessary for the enzyme to reach full activity becomes shorter (20). It is clear that the lag for domain nucleation is not the only factor responsible for the lag time required to reach full catalytic capacity. A succession of processes, such as enzyme partitioning to the interface, association to the substrate, a bimolecular kinetic step, and a slow irreversible activation step, have been described to occur during the lag time period of SMase acting on substrate monolayers and are in part responsible for the lag time found against the SM/Cer (9:1) films (22).

CONCLUSIONS

According to Alexa-labeled SMase localization, substrate-product mixing-demixing state, and kinetic-topographic considerations, the results support an "area-activated mechanism" for SMase action on lipid monolayers in which the enzyme is homogeneously active over all the surface of the LE phase. A novel mechanism for the lag time regulation by the presence of LC domains is proposed on the basis of domain nucleation kinetic barriers. This is mainly contributed by the line tension in relation to a rather large compositional gap that appears, in part, to be responsible for the existence of the lag time necessary for SMase to reach a steady-state rate of SM degradation.

The surface topograpy appears to follow classical nucleation theory, being the SMase enzymatic activity only responsible as a perturbation factor driving the compositional change of the system through the rate of Cer production.

REFERENCES

1. Roberts, M. F. 1996. Phospholipases: structural and functional motifs for working at an interface. *FASEB J.* **10:** 1159–1172.
2. Jain, M. K., J. Rogers, D. V. Jahagirdar, J. F. Marecek, and F. Ramirez. 1986. Kinetics of interfacial catalysis by phospholipase A2 in intravesicle scooting mode, and heterofusion of anionic and zwitterionic vesicles. *Biochim. Biophys. Acta.* **860:** 435–447.
3. Maggio, B. 1994. The surface behavior of glycosphingolipids in biomembranes: a new frontier of molecular ecology. *Prog. Biophys. Mol. Biol.* **62:** 55–117.
4. Maggio, B. 1996. Control by ganglioside GD1a of phospholipase A2 activity through modulation of the lamellar-hexagonal (HII) phase transition. *Mol. Membr. Biol.* **13:** 109–112.
5. Bell, J. D., M. Burnside, J. A. Owen, M. L. Royall, and M. L. Baker. 1996. Relationships between bilayer structure and phospholipase A2 activity: interactions among temperature, diacylglycerol, lysolecithin, palmitic acid, and dipalmitoylphosphatidylcholine. *Biochemistry.* **35:** 4945–4955.
6. Huang, H. W., E. M. Goldberg, and R. Zidovetzki. 1996. Ceramide induces structural defects into phosphatidylcholine bilayers and activates phospholipase A2. *Biochem. Biophys. Res. Commun.* **220:** 834–838.

7. Grandbois, M., H. Clausen-Schaumann, and H. Gaub. 1998. Atomic force microscope imaging of phospholipid bilayer degradation by phospholipase A2. *Biophys. J.* **74:** 2398–2404.
8. Leidy, C., L. Linderoth, T. L. Andresen, O. G. Mouritsen, K. Jorgensen, and G. H. Peters. 2006. Domain-induced activation of human phospholipase A2 type IIA: local versus global lipid composition. *Biophys. J.* **90:** 3165–3175.
9. Grainger, D. W., A. Reichert, H. Ringsdorf, and C. Salesse. 1990. Hydrolytic action of phospholipase A2 in monolayers in the phase transition region: direct observation of enzyme domain formation using fluorescence microscopy. *Biochim. Biophys. Acta.* **1023:** 365–379.
10. Dahmen-Levison, U., G. Brezesinski, and H. Mohwald. 1998. Specific adsorption of PLA2 at monolayers. *Thin Solid Films.* **327–329:** 616–620.
11. Simonsen, A. C., U. B. Jensen, and P. L. Hansen. 2006. Hydrolysis of fluid supported membrane islands by phospholipase A2: time-lapse imaging and kinetic analysis. *J. Colloid Interface Sci.* **301:** 107–115.
12. Sanchez, S. A., L. A. Bagatolli, E. Gratton, and T. L. Hazlett. 2002. A two-photon view of an enzyme at work: *Crotalus atrox* venom PLA2 interaction with single-lipid and mixed-lipid giant unilamellar vesicles. *Biophys. J.* **82:** 2232–2243.
13. Hannun, Y. A., and C. Luberto. 2000. Ceramide in the eukaryotic stress response. *Trends Cell Biol.* **10:** 73–80.
14. van Blitterswijk, W. J., A. H. van der Luit, R. J. Veldman, M. Verheij, and J. Borst. 2003. Ceramide: second messenger or modulator of membrane structure and dynamics? *Biochem. J.* **369:** 199–211.
15. Fanani, M. L., and B. Maggio. 1998. Surface pressure-dependent cross-modulation of sphingomyelinase and phospholipase A2 in monolayers. *Lipids.* **33:** 1079–1087.
16. Ruiz-Arguello, M. B., M. P. Veiga, J. L. Arrondo, F. M. Goni, and A. Alonso. 2002. Sphingomyelinase cleavage of sphingomyelin in pure and mixed lipid membranes. Influence of the physical state of the sphingolipid. *Chem. Phys. Lipids.* **114:** 11–20.
17. Contreras, F. X., J. Sot, M. B. Ruiz-Arguello, A. Alonso, and F. M. Goni. 2004. Cholesterol modulation of sphingomyelinase activity at physiological temperatures. *Chem. Phys. Lipids.* **130:** 127–134.
18. Fanani, M. L., S. Hartel, R. G. Oliveira, and B. Maggio. 2002. Bidirectional control of sphingomyelinase activity and surface topography in lipid monolayers. *Biophys. J.* **83:** 3416–3424.
19. Hartel, S., M. L. Fanani, and B. Maggio. 2005. Shape transitions and lattice structuring of ceramide-enriched domains generated by sphingomyelinase in lipid monolayers. *Biophys. J.* **88:** 287–304.
20. De Tullio, L., B. Maggio, S. Hartel, J. Jara, and M. L. Fanani. 2007. The initial surface composition and topography modulate sphingomyelinase-driven sphingomyelin to ceramide conversion in lipid monolayers. *Cell Biochem. Biophys.* **47:** 169–177.
21. Bianco, I. D., and B. Maggio. 1989. Interactions of neutral and anionic glycosphingolipids with dilauroylphosphatidylcholine and dilauroylphosphatidic acid in mixed monolayers. *Coll. Surf.* **40:** 249–260.
22. Fanani, M. L., and B. Maggio. 2000. Kinetic steps for the hydrolysis of sphingomyelin by *Bacillus cereus* sphingomyelinase in lipid monolayers. *J. Lipid Res.* **41:** 1832–1840.
23. Calderon, R. O., B. Maggio, T. J. Neuberger, and G. H. De Vries. 1993. Surface behavior of axolemma monolayers: physico-chemical characterization and use as supported planar membranes for cultured Schwann cells. *J. Neurosci. Res.* **34:** 206–218.
24. Fanani, M. L., and B. Maggio. 1997. Mutual modulation of sphingomyelinase and phospholipase A2 activities against mixed lipid monolayers by their lipid intermediates and glycosphingolipids. *Mol. Membr. Biol.* **14:** 25–29.
25. Vanderlick, T. K., and H. Mohwald. 1990. Mode selection and shape transition of phospholipid monolayer domains. *J. Phys. Chem.* **94:** 886–890.
26. McConnell, H. M. 1990. Harmonic shape transitions in lipid monolayer domains. *J. Phys. Chem.* **94:** 4728–4731.
27. Jungner, M., H. Ohvo, and J. P. Slotte. 1997. Interfacial regulation of bacterial sphingomyelinase activity. *Biochim. Biophys. Acta.* **1344:** 230–240.
28. Grainger, D. W., A. Reichert, H. Ringsdorf, and C. Salesse. 1989. An enzyme caught in action: direct imaging of hydrolytic function and domain formation of phospholipase A2 in phosphatidilcholine monolayers. *FEBS Lett.* **252:** 73–82.
29. Evans, D. F., and H. Wennerstrom. 1999. The Colloidal Domain. 2nd edition. Wiley-VCH, New York.
30. Sugimoto, T. 2001. Monodispersed Particles. 1st edition. Elsevier Science B.V., Amsterdam.
31. Arnold, A., I. Cloutier, A. M. Ritcey, and M. Auger. 2005. Temperature and pressure dependent growth and morphology of DMPC/DSPC domains studied by Brewster angle microscopy. *Chem. Phys. Lipids.* **133:** 165–179.